We are IntechOpen,
the world's leading publisher of
Open Access books
Built by scientists, for scientists

4,800
Open access books available

122,000
International authors and editors

135M
Downloads

154
Countries delivered to

Our authors are among the

TOP 1%
most cited scientists

12.2%
Contributors from top 500 universities

CLARIVATE ANALYTICS
BOOK CITATION INDEX
INDEXED

WEB OF SCIENCE™

Selection of our books indexed in the Book Citation Index
in Web of Science™ Core Collection (BKCI)

Interested in publishing with us?
Contact book.department@intechopen.com

Application of Complex Wavelet Packet Transform (CWPT) in Coherent Optical OFDM (CO-OFDM) Communication Systems

Y. Ben-Ezra and B.I. Lembrikov

Additional information is available at the end of the chapter

http://dx.doi.org/10.5772/59054

1. Introduction

Coherent optical orthogonal frequency division multiplexing (CO-OFDM) is a modulation format that attracted wide interest due to its high spectral efficiency (SE) and robustness against chromatic dispersion (CD) and polarization mode dispersion (PMD). CO-OFDM communication systems with coherent detection combine high SE and high receiver sensitivity [1], [2]. CO-OFDM transmission at 1 Tb/s can be realized [1]. OFDM is implemented using fast Fourier transform (FFT) which results in inter carrier interference (ICI) and inter symbol interference (ISI) [1], [2]. Usually, in order to avoid ICI and ISI, a so-called cyclic prefix (CP) is inserted into OFDM symbols. The addition of CP requires an increase of a bandwidth and sampling rate of analog-to-digital converter (ADC) and digital-to-analog converter (DAC) decreasing SE [1], [2]. The need for CP can be avoided if the wavelet packet transform (WPT) is used in CO-OFDM systems instead of Discrete Fourier Transform (DFT) and inverse DFT (IDFT) [2]. In such a case, a signal can be expanded in an orthogonal set of so-called wavelets [1], [2]. WPTs provide orthogonality between OFDM subcarriers based on the wavelets instead of sinusoids. Wavelets have finite length. For this reason, wavelet transforms (WTs) have both frequency and time localization. It has been shown that WPT-OFDM single-polarization system can mitigate CD of 3380 ps/nm at bit rate of 112 Gb/s [1].

An alternative real-time multiplexing technique characterized by a high SE is the Nyquist wavelength division multiplexing (N-WDM) [3]. N-WDM is made up of temporal sinc-pulses [3]. Electrically generated Nyquist pulses are shaped with finite duration impulse response (FIR) filters, have nearly rectangular spectra, and are transmitted in independent WDM channels [3]. For the higher order filters the spectrum approaches to a rectan-

gle, and the inter channel guard bands can be kept small without introducing ICI [3]. N-WDM has been investigated both theoretically and experimentally [3], [4]. For the polarization-multiplexed quadrature phase-shift keying (PM-QPSK) transmitter based on two QPSK integrated modulators in nonreturn-to-zero (NRZ) modulation regime, and standard single mode fiber (SSMF) with the typical values of parameters such as bit rate of 111 Gb/s per channel, loss 0.22dB/km, dispersion 16.7 ps/nm/km, noise-figure 5 dB, BER=4×10^{-3} *at* the maximum distance of 2300 km, performance of CO-OFDM and N-WDM techniques appeared to be similar [3],[4].

Recently, dual-polarization transmission has been investigated as a promising technique for future high bit rate communication systems [1], [5]. In such a case, the optical fiber two-input two-output channel model is described by a two-element Jones vector for any OFDM symbol on a subcarrier [6]. In Fourier transform (FT) based optical OFDM (FTO-OFDM), individual subcarriers are single-sideband, and the phase dispersion caused by CD and PMD can be compensated. In WPT-OFDM systems, on the contrary, the modulated signals are double-sideband. Unlike CD, PMD does not possess the phase symmetry [5]. Consequently, the Jones matrixes for the positive and negative sidebands are not equal, the dispersions of the two sidebands are different, and their addition does not represent the initial real WT basis. As a result, the orthogonality is broken, and inter-packet-interference occurs [7].

We proposed a novel type of CO-OFDM based on the dual-tree complex WPT (DT-CWPT) recently developed by N. Kingsbury [7]. DT-CWPT utilizes two wavelet filter banks (FBs) [8].

1. A first wavelet FB is used in the discrete WT (DWT).

2. A second wavelet FB is constructed in such a way that its impulse responses are approximately the discrete Hilbert transforms of the first wavelet FB.

The first and the second FBs are the real and imaginary parts of the DT-CWPT, respectively. We have shown that PMD can be compensated by digital signal processing using a DT-CWPT. SE and the transmission distance are substantially increased. Numerical simulations show that the 1 Tb/s single-channel CO-OFDM transmission with high SE of 7.88 bit/s/Hz over the distance of 1800 km can be realized.

The proposed Chapter is constructed as follows. In Section 2, we discuss the fundamentals of CO-OFDM systems; in Section 3, the WPT based OFDM systems are considered; PMD influence on the CO-OFDM dual-polarization transmission is reviewed in Section 4. In Sections 5 and 6, the structure and the properties of CO-OFDM system based on DT-CWT and DT-CWPT are described, respectively. In Section 7, the original results are presented for the DT-CWPT based single-channel CO-OFDM transmission system including a laser-diode and Mach-Zehnder external modulator. We describe the methods of the CD, PMD, and nonlinearity mitigation and present the numerical simulations results. Conclusions are presented in Section 8.

2. Fundamentals of CO-OFDM systems

In this Section, we consider the fundamentals of CO-OFDM communication systems OFDM is a kind of multicarrier modulation (MCM) where the data information is carried over many lower rate subcarriers [9]. The block diagram of an OFDM system is shown in Fig. 1 [9].
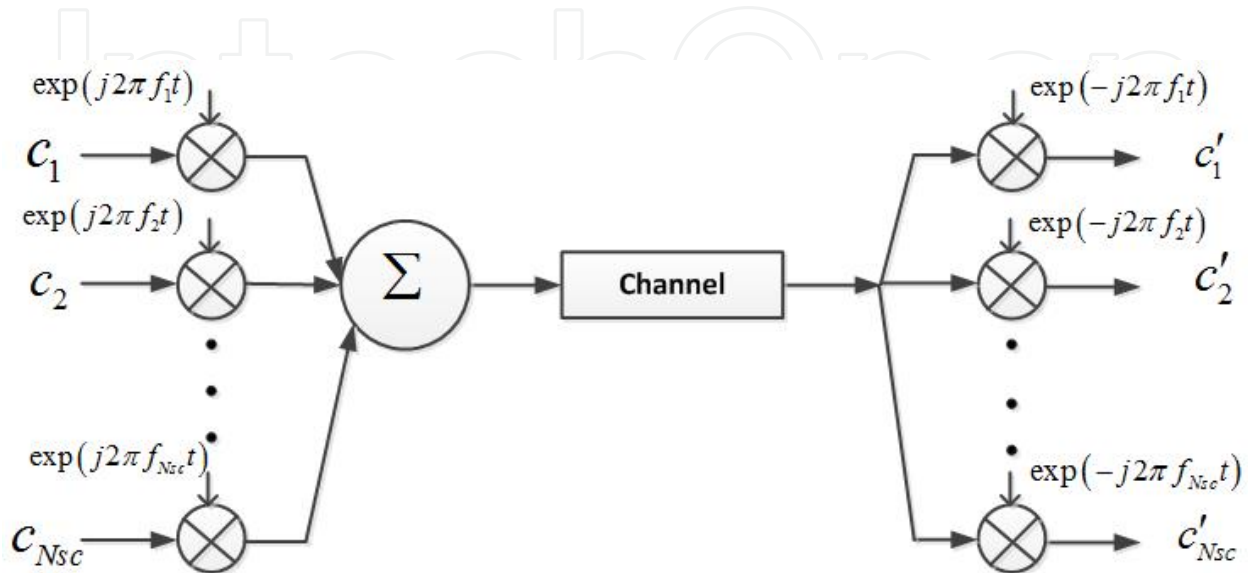

Figure 1. A diagram of OFDM system.

The fundamental advantages of OFDM are its robustness against channel dispersion and the ease of phase and channel estimation in a time-varying environment; the essential disadvantages of OFDM are high peak-to-average power ratio (PAPR) and sensitivity to frequency and phase noise [9]. The MCM transmitted signal is represented as follows [9].

$$s(t) = \sum_{i=-\infty}^{\infty} \sum_{k=1}^{N_{sc}} c_{ki} s_k (t - iT_s) \tag{1}$$

$$s_k(t) = \Pi(t)\exp(j2\pi f_k t) \tag{2}$$

$$\Pi(t) = \begin{cases} 1, & (0 < t \le T_s) \\ 0, & (t \le 0, t > T_s) \end{cases} \tag{3}$$

where c_{ki} is the i-th information symbol at the k-th subcarrier, s_k is the waveform for the k-th subcarrier, N_{sc} is the number of subcarriers, f_k is the frequency of the k-th subcarrier, T_s is the symbol period, and $\Pi(t)$ is the pulse shaping function. The detected information symbol c'_{ki} is given by [9].

$$c'_{ki} = \frac{1}{T_s} \int_0^{T_s} r(t - iT_s) \exp(-j2\pi f_k t) dt \qquad (4)$$

where $r(t)$ is the received time domain signal. In the case of the classical MCM nonoverlapped bandlimited signals are used which results in the excessive bandwidth and decrease of SE. In the case of OFDM, the overlapped orthogonal signal sets are determined by the following condition for any two orthogonal subcarriers [9].

$$\frac{1}{T_s} \int_0^{T_s} s_k s_l^* dt = \delta_{kl} \qquad (5)$$

Substituting expression (2) into (5) and carrying out the integration we obtain.

$$\exp\left[j\pi (f_k - f_l) T_s \right] \frac{\sin\left[\pi (f_k - f_l) T_s \right]}{\left[\pi (f_k - f_l) T_s \right]} = \delta_{kl} \qquad (6)$$

The orthogonality condition (6) is satisfied for the following relationship between the subcarrier frequencies

$$f_k - f_l = m \frac{1}{T_s}; m = 1, 2, ... \qquad (7)$$

In such a case, the orthogonal subcarrier sets can be recovered with the matched filters without ICI even for the strong signal overlapping [9]. OFDM modulation and demodulation can be implemented by using IDFT/DFT where the m-th samples s_m and r_m of the MCM transmitted and received signals $s(t)$ and $r(t)$, respectively, are given by [9].

$$s_m = \sum_{k=1}^{N} c_k \exp\left[j2\pi \frac{(k-1)(m-1)}{N} \right] = F^{-1}\{c_k\}; c'_k = F\{r_m\} \qquad (8)$$

Here $F\{r_m\}$ is the Fourier transform,

$m \in [1, N]$, $f_k = (k-1)/T_s; k \in [k_{min} + 1, k_{min} + N]$, k_{min} is an arbitrary integer, and T_s/N is the sampling interval. Expressions (8) show that the discrete value of the transmitted signal $s(t)$ is an N-point IDFT of the information symbol c_k, and the received information symbol c'_k is

an N-point DFT of the received sampled signal r_m [9]. The PAPR of the OFDM signal is given by the following expression [9]:

$$PAPR = \max\left\{\left|s(t)\right|^2\right\} / E\left\{\left|s(t)\right|^2\right\}, t \in \left[0, T_s\right] \tag{9}$$

where $\max\{|s(t)|^2\}$ and $E\{|s(t)|^2\}$ are the maximum value and the expectance of $|s(t)|^2$.

In order to implement IDFT/DFT DAC and ADC are needed. IDFT/DFT is characterized by two important advantages [9].

1. The computation complexity measured with the number of complex multiplications is reduced to $(N/2)\log_2(N)$ which is almost linear with respect to the subcarriers number N.

2. The OFDM system architecture is relatively simple. It does not require complex radio frequency (RF) oscillators and filters.

OFDM is characterized by the ISI and ICI as it was mentioned above. These phenomena are caused by a large number of subcarriers [9]. CP, i.e. the cyclic extension of the OFDM waveform into the guard interval (GI) Δ_G, has been proposed in order to prevent ISI and ICI [9]. If the GI is long enough to contain the intersymbol transition, then the remaining part of the OFDM symbol satisfies the orthogonality conditions (6), (7) and receiver cross-talk occurs only within GI [10]. The addition of CP requires an increase of a bandwidth and sampling rate of ADC and DAC. CP is an easily recognizable feature of an OFDM system which results in the signal vulnerability to interception by surveillance receiver [11]. Hence, the elimination of CP reduces the probability of interception and improves SE [11]. CP can be inserted implicitly into the definition of the MCM transmitted signal $s(t)$ (1)-(3) by modification of equation (3) which takes the form [9].

$$\Pi(t) = \begin{cases} 1, & \left(-\Delta_G < t \leq T_s\right) \\ 0, & \left(t \leq -\Delta_G, t > T_s\right) \end{cases} \tag{10}$$

OFDM is characterized by the dispersion robustness, high SE, possibility of linear and nonlinear impairment mitigation [9]. For this reason, OFDM appeared to be an attractive long-haul transmission format for the optical communication systems [9], [12], [13].

The optical communication systems can be divided into two groups. The first group is based on optical wireless, multimode fiber (MMF) systems and plastic optical fiber (POF) systems where the OFDM signal is represented by the intensity of the optical signal; the second group is based on the single mode fiber (SMF) techniques where the OFDM signal is represented by the optical field [13]. The first group uses the direct detection technique, while the second group uses the coherent detection technique [9]. The optical OFDM

systems based on the coherent detection are called CO-OFDM [9], [12]. A generic CO-OFDM system consists of five functional blocks: the RF OFDM transmitter, the RF-to-optical (RTO) up-converter, the optical channel, the optical-to-RF (OTR) down-converter, and the RF OFDM receiver with the coherent detector [12]. CO-OFDM manifests higher receiver sensitivity, SE, and robustness against polarization dispersion [9]. CO-OFDM can achieve high SE by overlapping subcarrier spectrum and at the same time avoiding interference by using coherent detection and signal set orthogonality [9], [12]. CO-OFDM communication systems are characterized by the linearity in RTO up-conversion and optical-to-RF (OTR) down-conversion [9], [12]. The electrical bandwidth requirements for the CO-OFDM transceiver can be greatly reduced by using direct up/down conversion which results in the low cost of the high-speed electronic circuits [9], [12]. SE η of the CO-OFDM system is given by [9], [12].

$$\eta = \frac{2R}{B_{OFDM}} \approx 2\alpha; \alpha = \frac{t_s}{T_s} \tag{11}$$

where $R = N_{sc}/T_s$ is the total symbol rate, $B_{OFDM} = (2/T_s) + (N_{sc}-1)/t_s$ is the OFDM bandwidth, $N_{sc} \gg 1$, the factor of 2 accounts for two light wave polarizations in the fiber, and t_s is the observation period.

CO-OFDM communication systems possess the following advantages as compared to the intensity modulation with direct detection (IM/DD) systems [14].

1. The shot-noise limited receiver can be achieved with a sufficient local oscillator (LO) power.

2. The frequency resolution at the intermediate frequency (IF) or baseband stage is high enough in order to separate close wavelength-division multiplexed (WDM) channels in the electric domain.

3. The phase detection improves the receiver sensitivity compared with IM/DD systems.

4. The advanced multilevel modulation formats can be introduced into optical communications by using phase modulation.

CO-OFDM communication systems can achieve high SE transmission through higher order modulation such as 64-QAM in single polarization and 16-QAM in dual polarization due to the DACs at the transmitter [9]. As a result, CO-OFDM techniques can be applied to the optical long-haul transmission at 100 Gb/s and beyond [9]. Recently, the 1.15 Tb/s no-guard-interval CO-OFDM (NGI-CO-OFDM) DP-QPSK superchannel transmission over the distance of 4520 km with SE=3.75b/s/Hz with BERs below the stringent forward error correction (FEC) limit has been demonstrated experimentally [15]. The pure silica core fiber and the erbium doped fiber amplifier (EDFA) have been used [15].

3. WPT based CO-OFDM systems

Conventional CO-OFDM systems based on DFT and IDFT can be replaced with WPT based CO-OFDM [1]. The sinusoidal functions are infinitely long in the time domain while wavelets have finite length being localized in time and in frequency domains [1]. Wavelet signal analysis can be a base for an effective computational algorithm which is faster and simpler than FFT [16]. Wavelets have been used in optical communications for time-frequency multiplexing and ultrafast image transmission [16]. A signal may be expanded in an orthogonal set of wavelet packets (WPs) as the basis functions, each channel occupies a wavelet packet (WP), and IDWPT/ DWPT are used at the transmitter and receiver, respectively [1], [16]. The theory and possible applications of continuous wavelet transform (CWT) and DWT are presented in [1], [16]-[19].

In particular, CO-OFDM system SE can be improved by avoiding CP. The problem of the CP elimination can be solved by using WPT-OFDM [16]. A mitigation of CD of 3380 ps/nm at 112 Gb/s without CP in the WPT-OFDM system has been demonstrated [1]. Typically, WPT-OFDM optical communication systems are single-polarization. However, the dual-polarization transmission is a promising technique for 1 Tb/s Ethernet transport [1]. Here we present some definitions and relationships essential for DWT applications.

CWT $W_T(a, \tau)$ of a given function $f(t)$ with respect to a mother wavelet (MW) $\psi(t)$ is defined as follows [17], [18]:

$$W_T\left(a,\tau\right) = \frac{1}{\sqrt{|a|}} \int_{-\infty}^{\infty} \psi^*\left(\frac{t-\tau}{a}\right) f(t) dt \qquad (12)$$

where the real numbers a and τ are the scaling and shifting, or translation parameters, respectively, and asterisk means complex conjugation. Note that in many practically important cases MW $\psi(t)$ is real. The functions $\psi^{a,\tau}(s) = |a|^{-1/2}\psi((s-\tau)/a)$ are called wavelets [18]. The set of wavelets is orthogonal and can be used as a basis instead of sinusoidal functions [16]. It is possible to localize the events described by $f(t)$ in time and frequency domains simultaneously by means of WT choosing the appropriate values of the parameters a and τ [17].

DWT is given by [17], [18]

$$W_T^{m,n}\left(a,\tau\right) = a_0^{-m/2} \int_{-\infty}^{\infty} \psi^*\left(a_0^{-m}t - n\tau_0\right) f(t) dt \qquad (13)$$

where $m, n \in Z$, Z is the set of all integers, and the constants $a_0 > 1$, $\tau_0 > 1$. Comparison of eqs. (12) and (13) shows that $a = a_0^m$ and $\tau = n\tau_0 a_0^m$ [17]. The orthogonal wavelet series expansions can be successfully used in DSP and multiplexing when the scaling and translation parameters

are discrete [17]. In such a case, a signal $s(t) \in V_0$ can be represented by a smooth approximation at resolution 2^M, obtained by combining translated versions of the basic scaling function $\phi(t)$, and M details at the dyadic scales $a = 2^l$, $(l = 1, 2, ..., M-1)$ obtained by combining shifted and dilated versions of the MW $\psi(t)$ as follows [17].

$$s(t) = \sum_k 2^{-M/2} c_M[k] \phi\left(2^{-M}t - k\Delta\tau\right) + \sum_{l=1}^{M} \sum_k 2^{-l/2} d_l[k] \psi\left(2^{-l}t - k\Delta\tau\right) \tag{14}$$

Here a subspace $V_0 \in L^2(R)$, $L^2(R)$ is a the linear vector space of square integrable functions, $2^{-l/2}\phi\left(2^{-l}t - k\Delta\tau\right)$ and $2^{-l/2}\psi\left(2^{-l}t - k\Delta\tau\right)$ are the orthonormal bases for the subspaces $V_l \in L^2(R)$ and $W_l \in L^2(R)$, respectively, $V_l \perp W_l$, $(l, k) \in Z$, $c_l[k]$ and $d_l[k]$ are the scaling and detail coefficients, respectively, at resolution 2^l, $\Delta\tau$ is the time interval coinciding with the inverse of the free spectral range (FSR).
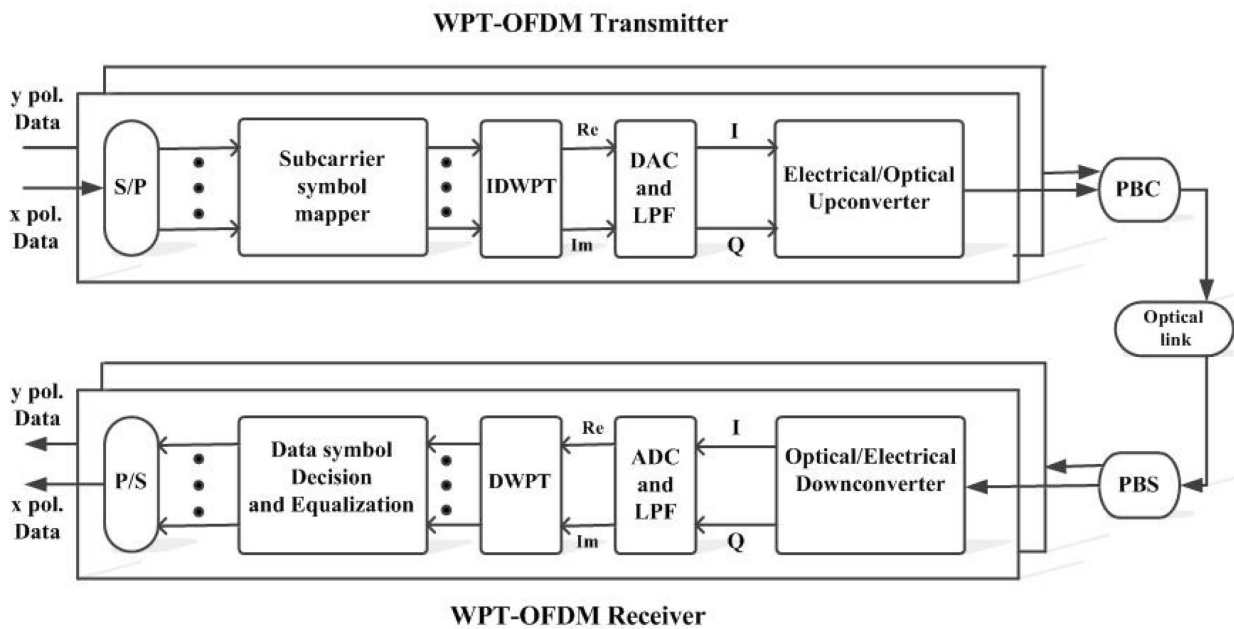

Figure 2. Block diagram of WPT-OFDM communication system. PBC/PBS: polarization beam Combiner/Splitter.

The block diagram of the WPT-OFDM communication system is shown in Fig. 2 [1]. In WPT-OFDM system each channel occupies a wavelet packet which plays a role of a subcarrier in wavelet domain. At the transmitter, IDWPT reconstructs the time domain signal from wavelet packets [1]. At the receiver, DWPT is used for the decomposition of the time domain signal into wavelet packets. The decomposition is carried out by means of successive low-pass and high-pass filtering in the time domain [1]. For WPT-OFDM, the basis function wavelets are finite in time, and the inter-symbol orthogonality in WT is caused by the shift orthogonal property of the waveforms [1], [17], [18]. In WT, symbols are overlapped in time domain [1].

As a result, the symbol duration increases. The symbol duration increase, in turn, provides the CD tolerance and eliminates the need for CP [1].

Real-valued wavelets are used for the real signal processing [1]. However for fiber optic channels, the up-conversion to the optical domain generates two spectral sidebands: a positive sideband and a negative one [1], [5]. In such a case, PMD influence on WT-OFDM is essential. It will be considered in Section 4.

4. PMD influence on the CO-OFDM communication system performance

In this Section we consider PMD in CO-OFDM communication systems and its influence on their performance [1], [5], [6], [9]. CO-OFDM transmission system can be defined as 2×2 multiple-input multiple-output (MIMO)-OFDM channel in the presence of polarization dispersion effects [7]. SMF supports two degenerate modes of orthogonal polarization [9]. However, the degeneracy may be broken due to the asymmetry in fiber geometry caused by the manufacture process or mechanical stress [9]. In such a case, a fiber birefrigence $B = |n_x - n_y|$ occurs where $n_{x,y}$ are the refractive indices for x and y polarization, respectively [9]. An optical signal with the wavelength λ propagating through the SMF is coupled from one polarization to the other with the coupling period $L_B = \lambda / B$ [9]. Typical values of these parameters are $B \approx 10^{-7}$, $L_B \approx 10m$ at $\lambda = 1.5 \mu m$ [9]. Then, the transmitted OFDM time-domain signal $s(t)$ (1) and the i-th information symbol at the k-th subcarrier c_{ki} (2) should be replaced with the Jones vectors for the two polarizations given by [6], [9].

$$s(t) = \begin{pmatrix} s_x \\ s_y \end{pmatrix}; \vec{c}_{ki} = \begin{pmatrix} c_{ki}^x \\ c_{ki}^y \end{pmatrix} \tag{15}$$

GI Δ_G in such a case must be long enough in order to handle the fiber CD and PMD. It takes the form [6], [9].

$$\Delta_G \geq \frac{c}{f^2} |D_t| N_{sc} \Delta f + (DGD)_{max} \tag{16}$$

where c is the speed of light, f is the optical carrier frequency, D_t is the total accumulated CD in units of ps/pm, Δf is the subcarrier channel spacing, and $(DGD)_{max}$ is the maximum budgeted differential-group-delay (DGD) which is typically chosen to be of 3.5 times of the mean PMD in order to satisfy inequality (16). The Jones vector of the received symbol $\vec{c}'_{ki} = (c'_{ki}x, c'_{ki}y)^t$ with a sufficiently long symbol period for the k-th subcarrier in the i-th OFDM symbol is given by [6], [9].

$$\vec{c}'_{ki} = \exp\left(j\phi_i\right)\exp\left(j\Phi_D\left(f_k\right)\right)T_k\vec{c}_{ki} + \vec{n}_{ki} \tag{17}$$

where $\vec{n}_{ki} = \left(n_{ki}^x, n_{ki}^y\right)^t$ is the noise including two polarization components, ϕ_i is the OFDM symbol phase noise, or common phase error (CPE) caused by the phase noises from the lasers and RF LOs at the transmitter and receiver, $\Phi_D(f_k) = \pi c D_t f_k^2 / f^2$ is the phase dispersion caused by the fiber CD, $T(k)$ is the Jones matrix for the fiber link given by [6], [9].

$$T(k) = \prod_{l=1}^{N}\exp\left\{\left(-\frac{1}{2}j\vec{\beta}_l f_k - \frac{1}{2}\vec{\alpha}_l\right)\bullet\vec{\sigma}\right\} \tag{18}$$

N is the number of PMD and polarization dependent loss (PDL) cascading elements, $\vec{\beta}_l$ is the l-th element birefringence vector, $\vec{\alpha}_l$ is the l-th element PDL vector, and $\vec{\sigma}$ is the Pauli matrix vector.

The CO-OFDM system architecture in the fiber optic channel can be divided into four groups related to the number of the transmitters and receivers used in the polarization dimension [6], [9].

1. Single-input single-output (SISO) where one optical OFDM transmitter and one optical OFDM receiver are used for CO-OFDM transmission. The SISO configuration is susceptible to the polarization mode coupling in a fiber. It requires a polarization controller (PC) before the receiver in order to align the input signal polarization with the LO polarization. However, in the case of large PMD, PC cannot prevent the polarization rotation between subcarriers. As a result, SISO CO-OFDM is susceptible to polarization-induced fading and should not be implemented in applications.

2. Single-input two-output (SITO) where one optical OFDM transmitter and two optical OFDM receivers are used, one for each polarization. In such a system, PC is not needed. SITO CO-OFDM system is resilient to PMD when the polarization diversity receiver is used. The PMD in the fiber link may even improve the system margin against PDL-induced fading.

3. Two-input single-output (TISO) where two optical OFDM transmitters and one optical OFDM receiver are used. This time, each transmitter is used for one specified polarization. The PC is not needed at the transmit end. The polarization diversity transmitter can achieve PMD resilience. In the TISO scheme, the same information symbol is repeated in two consecutive symbols which results in the electrical and optical efficiency reducing by half and the two times increase of the optical signal-to-noise ratio (OSNR) requirement as compared to SITO scheme.

4. Two-input two-output (TITO) where a polarization diveristy optical OFDM transmitter and a polarization diveristy optical OFDM receiver are used. In such a scheme, the transmitted OFDM information symbol c_{ik} is considered as polarization modulation or

polarization multiplexing. Hence, the channel capacity is doubled as compared to the SITO scheme. The PMD rotates subcarrier polarization and does not influence the channel capacity doubling. In the case of the TITO scheme, the polarization diversity receiver permits to avoid the polarization tracking at the receiver.

Comparison of the properties of the different CO-MIMO-OFDM architectures shows that SITO-and TITO-OFDM are the preferred configurations [9].

Consider the PMD influence on the transmission in a 2x2 MIMO CO-OFDM system. In such a case, the Jones matrix (18) for the fiber link on the k-th subcarrier in the first-order PMD approximation is given by [1], [5].

$$T(k) = M^{-1} \begin{bmatrix} \exp(-j\pi f_k \tau_{link}) & 0 \\ 0 & \exp(j\pi f_k \tau_{link}) \end{bmatrix} M \tag{19}$$

where τ_{link} is the DGD of the link, and the matrix M has the form.

$$M = \begin{bmatrix} \cos\left(\dfrac{\theta}{2}\right)\exp\left(-j\dfrac{\varphi}{2}\right) & -\sin\left(\dfrac{\theta}{2}\right)\exp\left(-j\dfrac{\varphi}{2}\right) \\ \sin\left(\dfrac{\theta}{2}\right)\exp\left(j\dfrac{\varphi}{2}\right) & \cos\left(\dfrac{\theta}{2}\right)\exp\left(j\dfrac{\varphi}{2}\right) \end{bmatrix} \tag{20}$$

Here θ, φ are the polar and azimuth angle of the principle state of polarization. In FTO-OFDM systems, the individual subcarrier is single-sideband by nature, and $\Phi_D(f_k)$, $T(k)$ can be estimated and compensated [5]. In WT based OFDM systems the modulated signals are double-sideband as it was mentioned above. CD influence on such a system is insignificant since the two sidebands have the same phase dispersion: $\Phi_D(f_k) = \Phi_D(-f_k)$. On the contrary, PMD does not have phase symmetry: $T(k) \neq T(-k)$. As a result, at the receiver two sidebands experience two different dispersions, and their addition does not reproduce the real wavelet basis, the orthogonality is broken, and the inter-packet-interference occurs [1], [5]. The WPT-OFDM systems are more susceptible to PMD then conventional FT-OFDM systems [1], [5].

5. Dual-Tree Complex Wavelet Transform (DT-CWT)

DWT has two main disadvantages [7], [8].

1. It is not shift-invariant. For this reason, the small shift in the input signal can cause major variations in the energy distribution between DWT coefficients at different scales.

2. It is characterized by a low directional selectivity for the diagonal elements since the wavelet filters are separable and real.

The DT-CWT has been proposed recently [7], [8]. DT-CWT consists of two WTs operating in parallel on an input signal [8]. In order to construct a DT-CWT, each sub band should be repeatedly decomposed using low-pass/high-pass PR FBs [8]. The response of each branch of the second WP FB is the discrete Hilbert transform of the corresponding branch of the first WP FB [8]. These WTs correspond to two FBs. The block diagram of DT-CWT is shown in Fig. 3 [8].
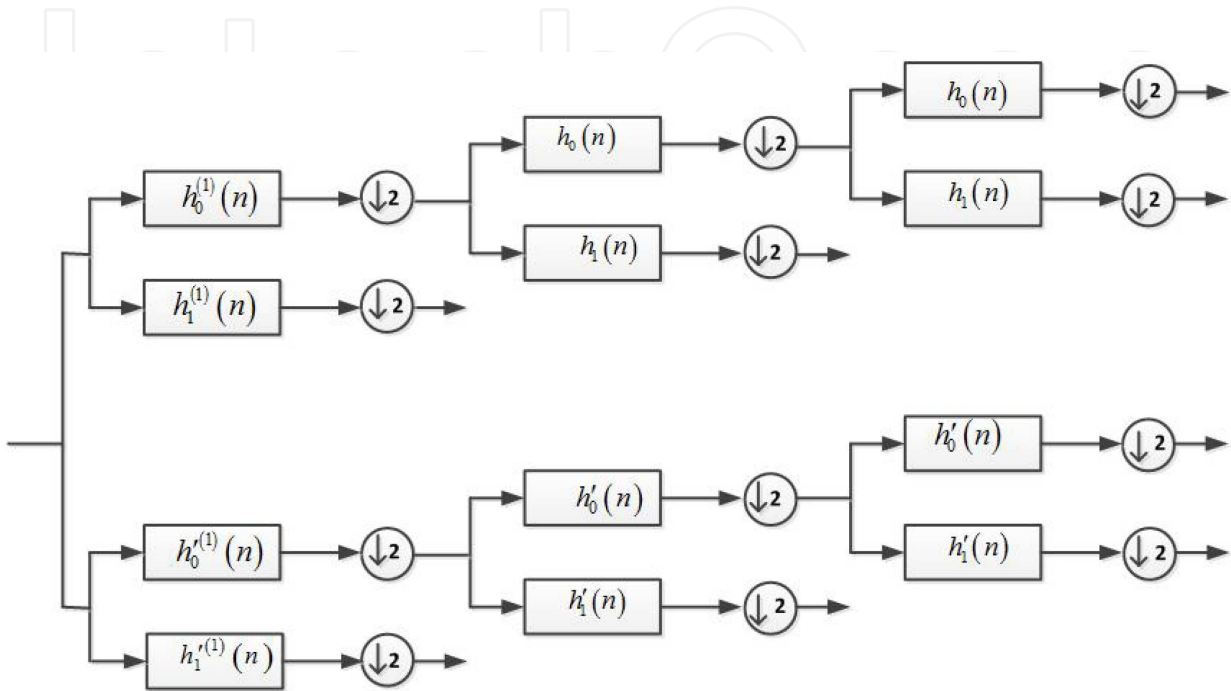

Figure 3. The DT-CWT consists of two wavelet FBs operating in parallel.

The first wavelet FB is determined by DWTs, the second FB contains the discrete Hilbert transforms of the first wavelet FB [8]. The first FB is the real part and the second FB is the imaginary part of the CWPT [8].

The wavelet function $\psi(t)$ associated with the first FB and the corresponding scaling function $\phi(t)$ have the form [8].

$$\psi(t) = \sqrt{2}\sum_{n} h_1(n)\phi(2t - n); \phi(t) = \sqrt{2}\sum_{n} h_0(n)\phi(2t - n) \tag{21}$$

For an orthonormal wavelet basis, the LPFs and high-pass filters (HPFs) have the following relationships $H_1(e^{j\omega}) = -e^{-j\omega d}H_0^*(e^{j(\omega-\pi)})$, or equivalently $h_1(n) = (-1)^n h_0(d - n)$ where d is an odd integer [8]. The wavelet function $\psi'(t)$ and the filters $h'_0(n)$, $h_1'(n)$ for the DT-CWPT imaginary part are defined in a similar way [6]. The filters $\{h_0(n), h_1(n)\}$ and $\{h'_0(n), h'_1(n)\}$ are assumed to be finite impulse response (FIR) conjugate quadrature filter (CQF) pairs [8]. In the case of the ideal DT-CWT we have.

$$\psi_c(t) = \mathrm{H}_{Hilbert}\{\psi(t)\} \tag{22}$$

where $H_{Hilbert}\{\psi(t)\}$ is the Hilbert transform of $\psi(t)$ and the complex wavelet $\psi(t) = \psi(t) + j\psi'(t)$ is approximately analytic [20]. In order to satisfy the perfect reconstruction (PR) conditions, the filters are designed in such way that the two low pass filters (LPFs) should satisfy the half-sample delay condition: $h'_0(n) \approx h_0(n - 0.5)$ [20]. If each wavelet $\psi(t)$, $\psi'(t)$ are orthogonal to their integer translates, then the Hilbert relation between them is satisfied under the condition [8]:

$$H'_0(\exp(j\omega)) = \exp(-j0.5\omega)H_0(\exp(j\omega)), |\omega| < \pi \tag{23}$$

Then, for the HPFs we have [8]

$$H'_1(\exp(j\omega)) = -j\,\mathrm{sgn}(\omega)\exp(j0.5\omega)H_1(\exp(j\omega)), |\omega| < \pi \tag{24}$$

Here sgn is the signum function, $H'_{0,1}(\exp(j\omega))$, $H_{0,1}(\exp(j\omega))$ are the z-transforms of $h'_{0,1}(n)$, $h_{0,1}(n)$ on the unit circle, respectively [8]. It can be shown that the first stage of the DT-CWT must be different from the following stages [8]. The equivalent response $H^{(k)}(\exp(j\omega))$ of the kth stage of the first FB terminated with $H_1(\exp(j\omega))$ for $k > 1$ is given by:

$$H^{(k)}(\exp(j\omega)) = H_1(\exp(j2^{k-1}\omega))\prod_{m=0}^{k-2}H_0(\exp(j2^m\omega)), |\omega| < \pi \tag{25}$$

The equivalent response $H'^{(k)}(\exp(j\omega))$ of the second FB's corresponding branch can be obtained by replacing H_i with H'_i given by [8]:

$$H'^{(k)}(\exp(j\omega)) = -j\,\mathrm{sgn}(\omega)\exp(j0.5\omega)H^{(k)}(\exp(j\omega)), |\omega| < \pi \tag{26}$$

which is equivalent to the relationship

$H'^{(k)}(\exp(j\omega)) = -\exp(j0.5\omega)H_{Hilbert}\{H^{(k)}(\exp(j\omega))\}$ [8]

DT-CWT has the following properties [7].

1. Approximately shift-invariance.

2. Good directional selectivity in 2 dimensions.

3. Perfect reconstruction (PR) using short linear-phase filters.

4. Limited redundancy.

5. Efficient order-N computation.

6. Dual-Tree Complex Wavelet Packet Transform (DT-CWPT)

DT-CWT can be generalized to DT-CWPT by using the bases of discrete wavelet packet transforms (DWPTs). DT-CWPT is approximately shift-invariant, provides a geometrically oriented signal analysis in multiple dimensions and permits the transformation of a double-sideband spectrum into an approximately single-sideband one [7], [8]. The invert DT-CWPT is provided by the inversion of its real and imaginary parts [8].

The construction of the DT-CWPT requires the repeated decomposition of the sub bands by using low-pass/high-pass PR FBs [8]. The PR FBs should be chosen in such a way that the response of each branch of the second wavelet packet FB is the discrete Hilbert transform of the corresponding branch of the first wavelet packet FB [8]. Under this condition, each sub band of the DT-CWPT will be analytic [8]. Taking into account that the discrete Hilbert transform is a linear time-invariant (LTI) system we can write the following relationships for the discrete Hilbert transform pair of the filters $g(n)$, $h(n)$ [8].

$$G\left(\exp\left(j\omega\right)\right) = j\,\mathrm{sgn}\left(\omega\right)H\left(\exp\left(j\omega\right)\right), |\omega| < \pi \qquad (27)$$

$$G\left(\exp\left(j\omega\right)\right)C\left(\exp\left(j\omega\right)\right) = j\,\mathrm{sgn}\left(\omega\right)H\left(\exp\left(j\omega\right)\right)C\left(\exp\left(j\omega\right)\right), |\omega| < \pi \qquad (28)$$

Then, the convolutions $g(n) * c(n)$, $h(n) * c(n)$ are also a discrete Hilbert transform pair [8].

It has been shown that a DT-CWPT consisting of two wavelet packet FBs operating in parallel can be produced where some filters in the second wavelet packet FB are the same as those in the first wavelet packet FB [8].

The first of these two wavelet FBs for a four-stage DT-CWPT is shown in Fig. 4 [8]. The second wavelet packet FB is obtained by replacing the first stage filters $h_i^{(1)}(n)$ with $h_i^{(1)}(n-1)$ and by replacing $h_i(n)$ with $h'_i(n)$ for $i \in \{0, 1\}$ [8]. The filters F_i are unchanged in the second wavelet packet FB [8].

In order to demonstrate the development of the M-band DT-CWT based on the Hilbert pairs of M-band wavelets, consider the construction of the four-band DT-CWT (M=4) from a given two-band DT-CWT which is defined by a two-channel orthonormal FB $\left\{h_0^{(2)}(n), h_1^{(2)}(n)\right\}$ associated with the scaling function $\phi^{(2)}(t)$ and the wavelet $\psi^{(2)}(t)$ [8]. Their Fourier transforms (FTs) have the form [8].
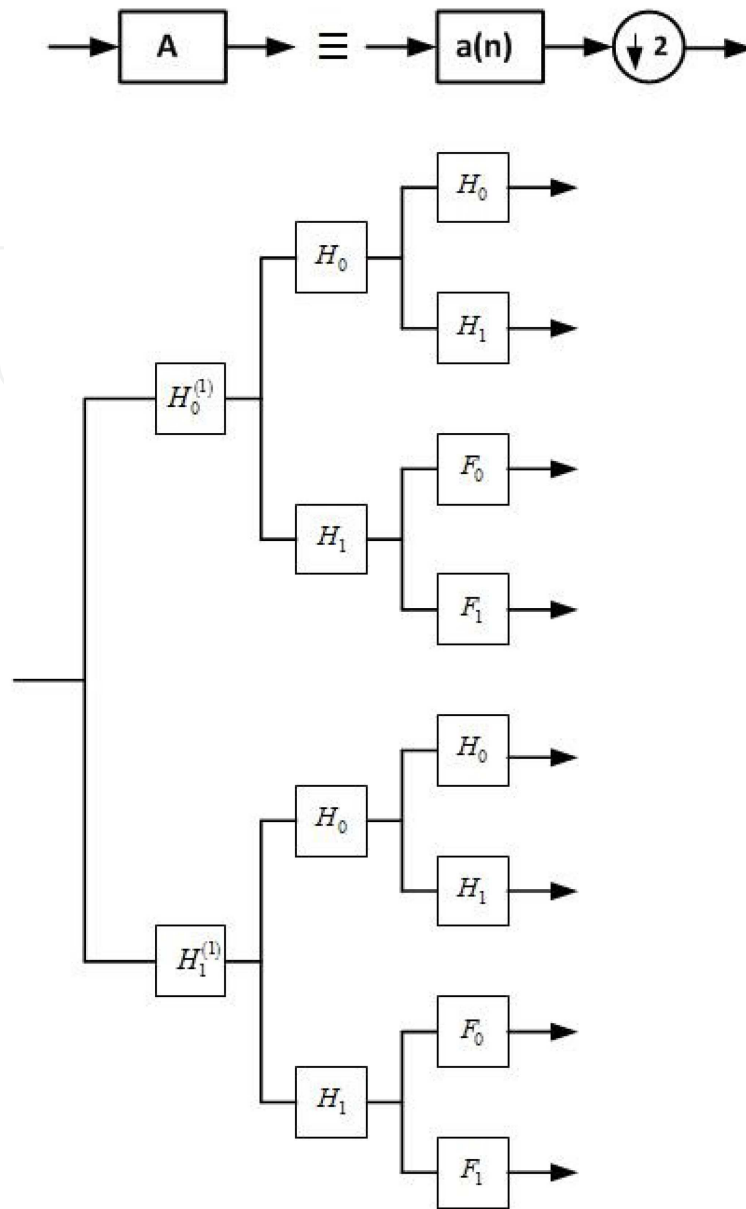
Figure 4. First wavelet packet FB of a four-stage DT-CWPT.

$$\Phi^{(2)}(\omega) = \prod_{l=1}^{\infty} \left[\frac{1}{\sqrt{2}} H_0^{(2)}\left(\frac{\omega}{2^l}\right) \right]; \Psi^{(2)}(\omega) = \frac{1}{\sqrt{2}} H_1^{(2)}\left(\frac{\omega}{2}\right) \Phi^{(2)}\left(\frac{\omega}{2}\right) \tag{29}$$

A two-band DT-CWT can be created if we have a second two-channel orthonormal FB $\{h_0'^{(2)}(n), h_1'^{(2)}(n)\}$ with the associated scaling function $\phi'^{(2)}(t)$ and the wavelet $\psi'^{(2)}(t) = H_{Hilbert}\{\psi^{(2)}(t)\}$, where the complex wavelet $\psi^{(2)}(t) + j\psi'^{(2)}(t)$ is analytic [8]. In order to construct a four-band CWT, another two-channel orthonormal FB $\{f_0(n), f_1(n)\}$ is necessary [8]. The corresponding four-channel orthonormal FB, i.e a DWPT is shown in Fig. 5 [8].
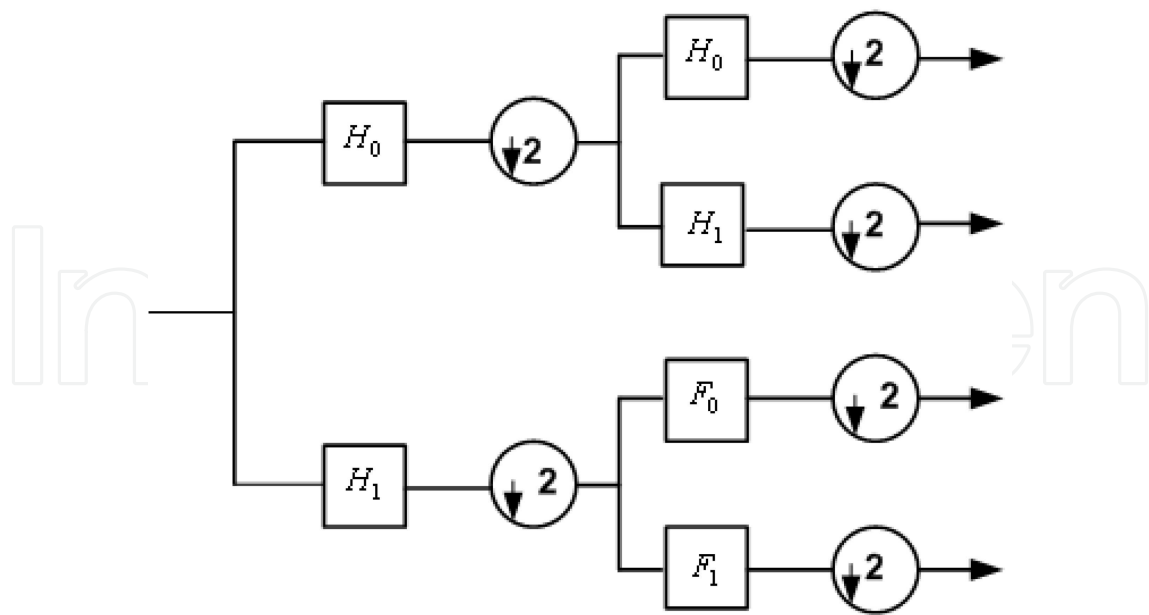
Figure 5. Discrete wavelet packet transform (DWPT).

A second WPT such that the wavelets associated with the two WPTs form the Hilbert transform pairs is given by [8].

$$H_0^{(4)}\left(\exp(j\omega)\right) = H_0^{(2)}\left(\exp(j\omega)\right) H_0^{(2)}\left(\exp(j2\omega)\right) \tag{30}$$

$$H_1^{(4)}\left(\exp(j\omega)\right) = H_0^{(2)}\left(\exp(j\omega)\right) H_1^{(2)}\left(\exp(j2\omega)\right) \tag{31}$$

$$H_2^{(4)}\left(\exp(j\omega)\right) = H_1^{(2)}\left(\exp(j\omega)\right) F_0\left(\exp(j2\omega)\right) \tag{32}$$

$$H_3^{(4)}\left(\exp(j\omega)\right) = H_1^{(2)}\left(\exp(j\omega)\right) F_1\left(\exp(j2\omega)\right) \tag{33}$$

It can be shown that the FB determined by eqs. (30)-(33) is equivalent to the FB shown in Fig. 5 [8].

7. Simulation results for the single channel DT-CWPT based CO-OFDM system

We have carried out the numerical simulations based on DT-CWPT for the single-channel CO-OFDM transmission system including the optical front elements such as a laser-diode, and

Mach-Zehnder external modulator [21]. The nonlinear effects are neglected since Hilbert transform is LTI system [8]. We used the 16 quadrature amplitude modulation (QAM) with $128=2^7$ sub bands, 7 decomposition levels, bit rate of 100 Gb/s and the bandwidth of 25 GHz. The typical values of transmission process are following: the input optical signal power is equal to 10 mW; CP is 1%; the phase noise frequency in the case of the coherent detection is equal to 500 KHz; the overall noise amplification level of the link is 50 dB; the pre-amplifier gain at the receiver input is 25 dB; the optical fiber dispersion constant is 17 $ps/(nm \cdot km)$; the PMD constant is 0.1 ps/km$^{1/2}$. The 8 bit DAC and ADC have been used. In order to mitigate the group velocity dispersion and PMD we used the Least Mean Square (LMS) and Viterbi-Viterbi Digital Signal Processing (DSP) algorithms [22]. We used in our simulations the complex wavelets based on the Q-shift filters [7], [8], [23]. The design of pairs of wavelet bases where the wavelets form a Hilbert transform pair was also discussed in detail in [24], [25]. The numerical simulation results are presented in Figs. 6-11. The QAM-16 modulated signal constellations for the transmission distance of 100 km, 700 km and 1700 km in the case of the DT-CWPT based CO-OFDM system are shown in Figs.6-8, respectively.

The QAM-16 modulated signal constellations for the transmission distance of 1200 km and 1300 km in the case of the conventional CO-OFDM system are shown in Figs.9-10, respectively. In both cases CP=1% has been used.
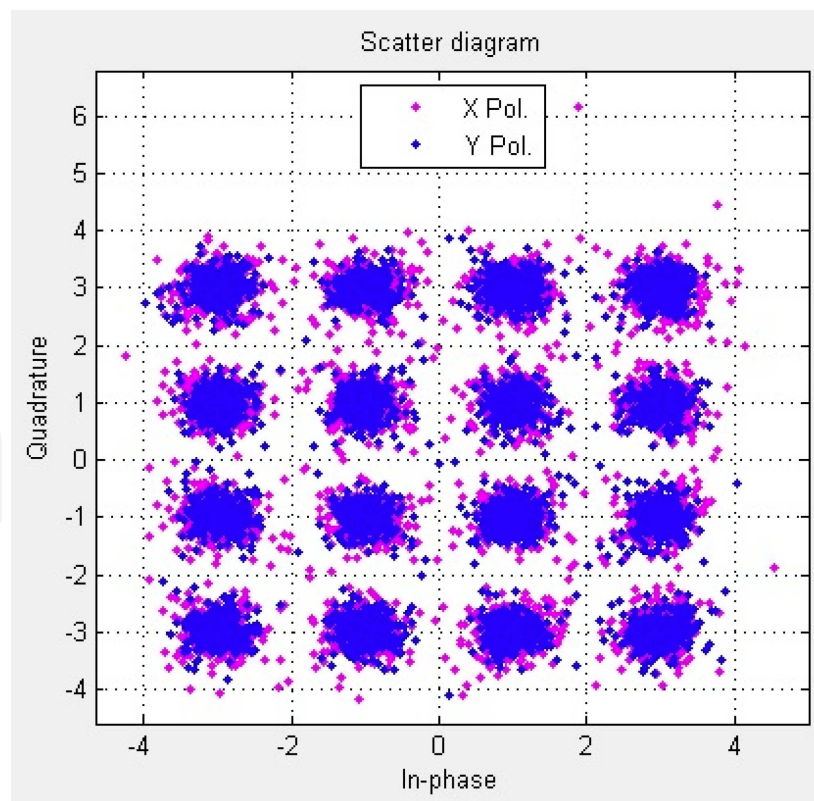

Figure 6. The QAM-16 modulated signal constellation for the transmission distance of 100 km, CP 1%, BER=10$^{-2.56}$, DT-CWPT based CO-OFDM system.
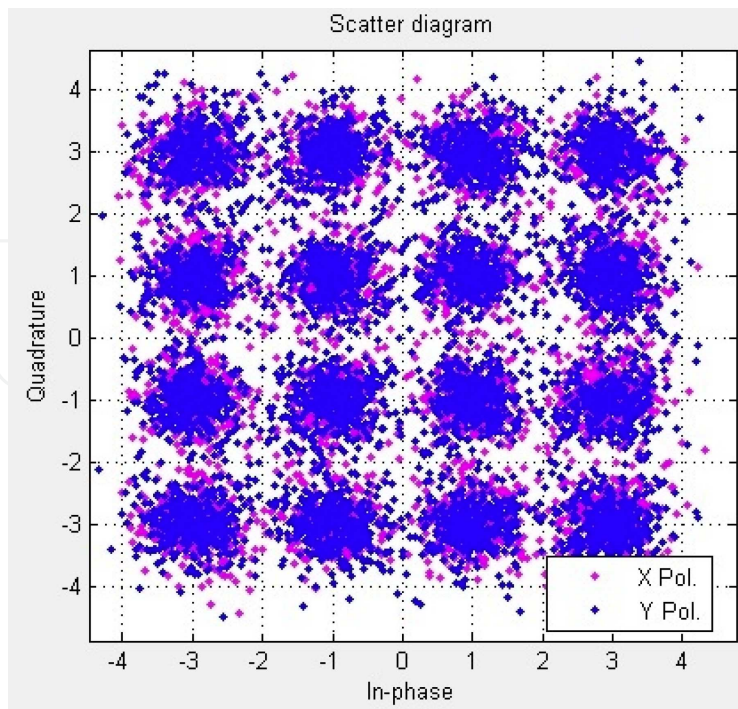
Figure 7. The QAM-16 modulated signal constellation for the transmission distance of 700 km, CP 1%, BER=$10^{-2.13}$, DT-CWPT based CO-OFDM system.
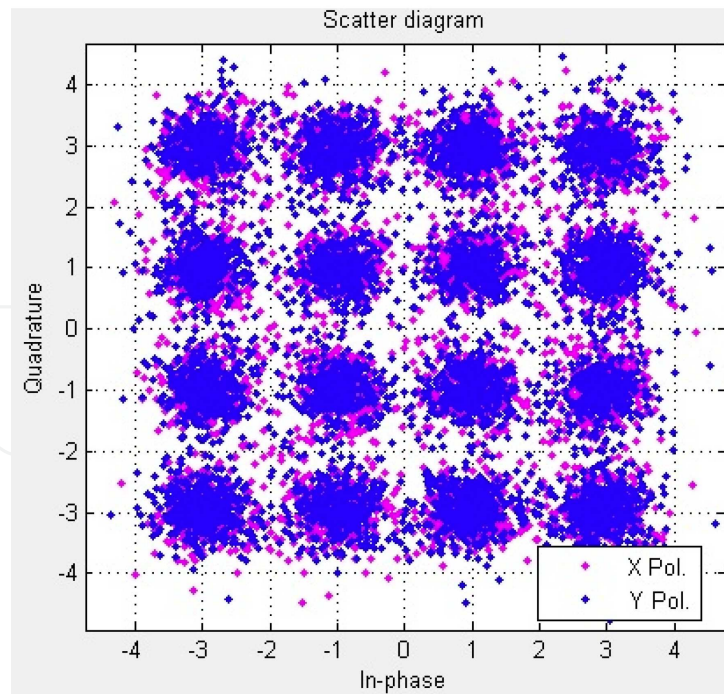

Figure 8. The QAM-16 modulated signal constellation for the transmission distance of 1700 km, CP 1%, BER=$10^{-2.08}$, DT-CWPT based CO-OFDM system.
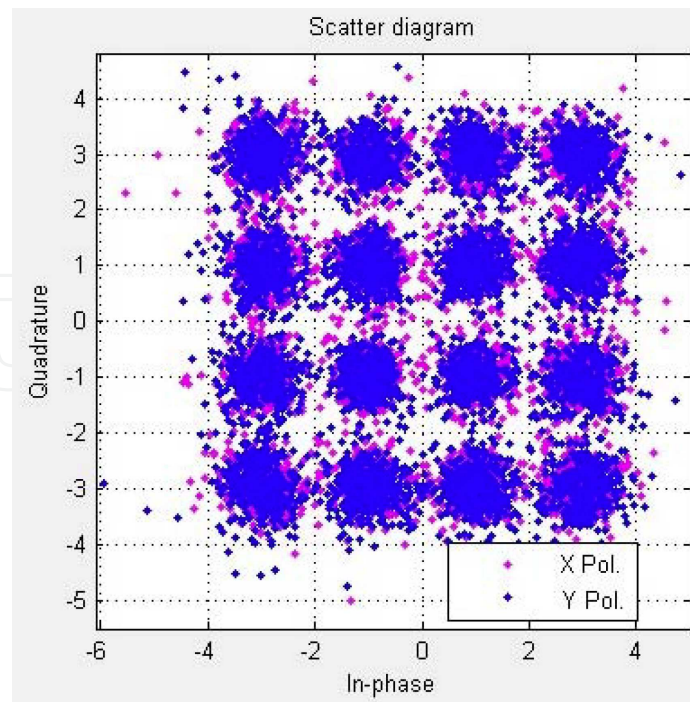
Figure 9. The QAM 16 modulated signal constellation for the transmission distance of 1200 km, BER=$10^{-2.08}$, CP 1% Conventional CO-OFDM system.
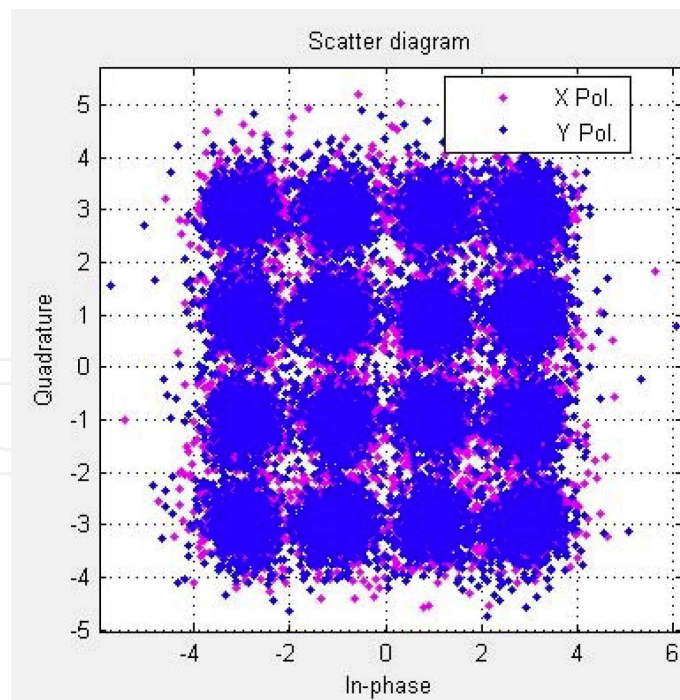

Figure 10. The QAM 16 modulated signal constellation for the transmission distance of 1300 km, BER=$10^{-1.83}$, CP 1% Conventional CO-OFDM system.

The QAM-16 modulated signal constellations for the transmission distance of 1200 km and 1300 km in the case of the conventional CO-OFDM system are shown in Figs.9-10, respectively. In both cases CP=1% has been used.

The comparison of Figs. 8 and 10 clearly shows that the performance of the DT-CWPT based OFDM communication system is better than the performance of the conventional CO-OFDM communication system. Indeed, for the same modulation format and CP, $BER = 10^{-1.83} = 1.48 \times 10^{-2}$ at the distance of 1300 km for the conventional CO-OFDM as compared to $BER = 10^{-2.08} = 8.32 \times 10^{-3}$ at the distance of 1700 km for the DT-CWPT based OFDM system.
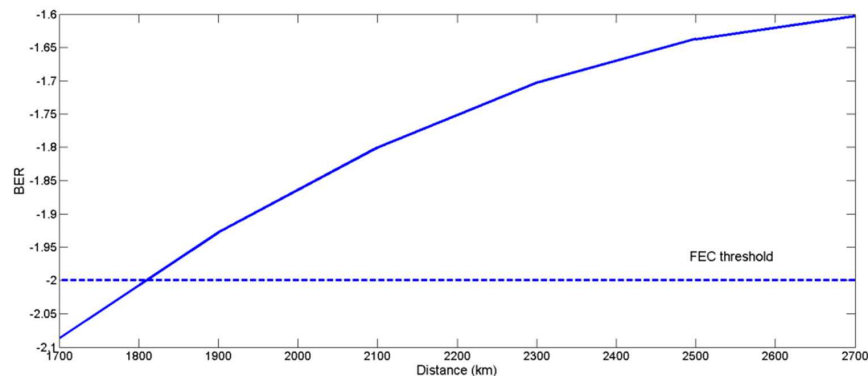

Figure 11. The BER dependence on the transmission distance for the DT-CWPT based CO-OFDM system.

The bit error rate (BER) dependence on the transmission distance for the DT-CWPT based CO-OFDM system is presented in Fig. 11. The forward error correction (FEC) threshold of BER=10^{-2} corresponds to the transmission distance of about 1800 km.

We have evaluated SE for the dual polarization signal, sampling rate of 26.6 GHz, and QAM 16 modulation format. The maximum available SE in such a case is 8bit/s/Hz. Assuming the FEC penalty of 20% per band, the CP penalty of 1.5%, and channel and timing estimation of 5%, we obtain the actual $SE = 8 \times 0.735 = 5.84 bit/s/Hz$.

8. Conclusions

CO-OFDM communication systems are characterized by high SE, possibility of the advanced modulation formats applications due to the coherent detection, and the high receiver sensitivity [1], [9], [13]. Conventional CO-OFDM systems are based on FTs [1], [9]. In such systems, low rate subcarriers are orthogonally transformed into time domain signals [1]. The condition of subcarrier orthogonality prevents spectral overlapping and ICI [1], [9]. The basis functions of the conventional CO-OFDM system are the infinitely long in time sinusoids. The 1-Tb/s CO-OFDM single-channel signal transmission over 600 km SSMF with SE of 3.3 bit/s/Hz and without Raman amplification and dispersion compensation has been reported [26]. In CO-

OFDM systems, the CD and PMD impairments can be compensated by choosing an appropriate length of CP [1], [9]. However, the CP insertion decreases the CO-OFDM communication system SE [1], [9].

Recently, the CO-OFDM systems based on WPTs have been proposed [1], [2]. Wavelets used as the basis functions in these advanced systems have finite length in the time domain. For this reason, WPT-OFDM systems do not need CP which results in a higher SE [1], [2]. The WPT-OFDM can mitigate a CD of 3380 ps/nm at 112 Gb/s rate without CP [1]. However, the high performance has been demonstrated for a CO-OFDM system based on a single-polarization [5]. The most promising technique for achieving high SE and maximizing power efficiency is coherent detection with polarization multiplexing where the in-phase (I) and quadrature (Q) signals are used in two field polarizations [27]. Information can be encoded in all available degrees of freedom, while the the compensation of transmission impairments can be provided by DSP [22], [27]. Advanced FEC coding can be also implemented [27]. Taking into account the importance of the polarization multiplexing, it is necessary to investigate the PMD influence on the dual-polarization transmission [5], [6].

In WPT-OFDM communication systems the modulated signals are double-sideband [5]. It has been shown that the CD influence on WPT-OFDM is compensated automatically due to the phase symmetry of the both sidebands while the PMD does not possess the phase symmetry [5]. As a result, the two sidebands have two different dispersions, their addition does not reproduce the real wavelet basis, orthogonality condition is broken, and inter-packet-interference occurs [5].

In this chapter, we considered the fundamentals of WPT based CO-OFDM communication systems and the PMD influence on such systems. It appeared to be that DT-CWPT can generate the single-sideband wavelets in frequency domain [5], [7], [8], [20], [21], [23]-[25]. We briefly discussed the properties of complex wavelets. The DT-CWPT consists of two real wavelet FBs where the second wavelet FB is the Hilbert transform of the first one and it represents an imaginary part of the CWT. The DT-CWPT approach to CO-OFDM communication systems mitigates the PMD impact on the system perfomance.

We have carried out the numerical simulations for the DT-CWPT based CO-OFDM system and QAM-16 modulation format. The constellation and BER dependence on the distance clearly show that the transmission over the distance of 1800 km with high actual **SE** of 5.85 bit/s/Hz taking into account the FEC and CP penalties, channel and timing estimation can be achieved due to the PMD mitigation provided by the DT-CWPT based CO-OFDM system.

We compared the performance of the conventional CO-OFDM and the DT-CWPT based CO-OFDM communication systems. The performance of the DT-CWPT based OFDM communication system is better than the performnace of the conventional CO-OFDM communication system: for the same modulation format and CP**,** BER at the distance of 1300 km for the conventional CO-OFDM is larger than BER at the distance of 1700 km for the DT-CWPT based OFDM system. We used in our simulations the already developed complex wavelets [23]-[25]. In future theoretical investigations, we suppose to find more appropriate wavelet bases using the so-called best-basis algorithms [8].

Author details

Y. Ben-Ezra and B.I. Lembrikov

Department of Electrical Engineering, Holon Institute of Technology, Holon, Israel

References

[1] Li An, Shieh W., and Tucker R.S. Wavelet packet transform-based OFDM for optical communications. Journal of Lightwave Technology, 2010; 28(24), 3519-3528.

[2] Ben Ezra Y., Lembrikov B.I., Zadok Avi, Ran Halifa R., and Brodeski D. All-optical Signal Processing for High Spectral Efficiency (SE) Optical Communication. In: Narottam Das (ed.) Optical Communication. Rijeka: InTech; 2012. p343-366.

[3] Schmogrow R., Bouziane R., Meyer M., Milder P.A., Schindler P.C., Killey R.I., Bayvel P., Koos C., Freude W., and Leuthold J. Real-time OFDM or Nyquist pulse generation – which performs better with limited resources? Optics Express 2012; 20(26) B543-B551.

[4] Bosco G., Carena A., Curri V., Poggiolini P., and Forghieri F. Performance limits of Nyquist-WDM and CO-OFDM in high-speed PM-QPSK systems. IEEE Photonic Technology Letters, 2010; 22(15) 1129-1131.

[5] Li An, Shieh W., and Tucker R.S. Impact of polarization-mode dispersion on wavelet transform based optical OFDM systems, In: proceedings of National Fiber Optic Engineers Conference, San-Diego, California, USA March 21-25, 2010, JThA5, pp.1-3.

[6] Shieh W., Yi X., Ma Y., and Tang Y. Theoretical and experimental study on PMD-supported transmission using polarization diversity in coherent optical OFDM systems. Optics Express 2007; 15(16) 9936-9947.

[7] Kingsbury N. Complex wavelets for shift invariant analysis and filtering of signals Journal of Applied and Computational Analysis 2001 10 (3) 234-253.

[8] Bayram I. and Selesnick I.W. On the dual-tree wavelet packet and M-band transforms. IEEE Transactions on Signal Processing 2008; 56(6) 2298-2310.

[9] Shieh W, Djordjevic I. Orthogonal Frequency Division Multiplexing for Optical Communications. London: Academic Press; 2010.

[10] Hillerkuss, D.et al. Simple all-optical FFT scheme enabling Tbit/s real-time signal processing, Optics Express, April 2010; 18(9) 9324-9340.

[11] Wang X.; Ho P., and Wu Y. Robust Channel Estimation and ISI Cancellation for OFDM Systems with Suppressed Features, IEEE Journal on Selected Areas in Communications 2005; 23(5) 963-972.

[12] Shieh W., Bao H., and Tang Y. Coherent optical OFDM: theory and design. Optics Express 2008; 16(2) 841-859.

[13] Armstrong J. OFDM for Optical Communications, IEEE Journal of Lightwave Technology, February 2009; 27(3) 189-204.

[14] Kikuchi K. Coherent optical communication systems, In: Kaminov, I. P.; Li, T. & Willner, A. E. (Eds.) Optical Fiber Telecommunications VB: Systems and Networks, Academic Press, Amsterdam, London, New York: Academic Press; 2008. p91-129.

[15] Da Silva E., Pataca D.M., Ranzini S. M., de Carvalho L.H.H., Juriollo A.A., da Silva M.L., Oliveira J.C.R.F. Transmission of 1.15 Tb/s NGI-CO-OFDM DP-QPSK super-channel over 4520 km of PSCF with EDFA-only amplification. Journal of Microwaves, Optoelectronics and Electromagnetic Applications, 2013; 12(SI-2) 96-103.

[16] Cincotti G., Moreolo M.S. and Neri A. Optical Wavelet Signals Processing and Multiplexing, EURASIP Journal on Applied Signal Processing, 2005; 10, 1574-1583.

[17] Rao R.M.& Bopardikar A. S. Wavelet Transforms. Introduction to Theory and Applications. Reading, Massachusetts: Addison-Wesley; 1998.

[18] Daubechies I. Ten Lectures on Wavelets. Philadelphia, Pennsylvania: Society for Industrial and Applied Mathematics; 2006.

[19] Sarkar K.T., Salazar-Palma M., Wicks M.C. Wavelet Applications in Engineering Electromagnetics. Boston: Artech House; 2002.

[20] Nerma M. H. M., Kamel N. S., Jeoti V. An OFDM based on dual tree complex wavelet transform (DT-CWT), Signal Processing: An International Journal (SPIJ), 2009; 3 (2) 14-26.

[21] Ben-Ezra Y., Brodeski D., Lembrikov B.I. High Spectral Efficiency OFDM Based on Complex Wavelet Packets. In: ICTON 2014: Proceedings of the 16th International Conference on Transparent Optical Networks, 6-10 July 2014, Graz, Austria, We.A1.4 p1-3.

[22] Kuschnerov M., Hauske F. N., Piyawanno K., Spinnler, B., Alfiad, M.S. Napoli, A., and Lankl, B. DSP for coherent single-carrier receivers, Journal of Lightwave Technology, 2009; 27(16) 3614-3622.

[23] Kingsbury N. Design of Q-shift complex wavelets for image processing using frequency domain energy minimization. In: Image Processing 2003. ICIP 2003. Proceedings of International Conference on Image Processing, 14-18 September 2003, Barcelona, Catalonia, Spain, 1, 1-1013-16.

[24] Kingsbury N. A dual-tree complex wavelet transform with improved orthogonality and symmetry properties. In: Image Processing 2000. ICIP 2000. Proceedings of International Conference on Image Processing, 10-13 September 2000, Vancouver, BC, Canada, 375-378.

[25] Selesnik I. W. Hilbert transform pairs of wavelet bases, IEEE Signal Processing Letters, 2001; 8(6) 170-173.

[26] Ma Y., Yang Q., Tang Y., Chen S., and Shieh W. 1-Tb/s single-channel coherent optical OFDM transmission over 600-km SSMF fiber with subwavelength bandwidth access. Optics Express 2009; 17(11) 9421-9427.

[27] Ip, Ezra, Lau, A.P.T., Barros, D.J.F., Kahn, J.M. Coherent detection in optical fiber systems. Optics Express, January 2008; 16(2) 753-791.